# NMR Analysis of Interaction of LqhαIT Scorpion Toxin with a Peptide Corresponding to the D4/S3−S4 Loop of Insect Para Voltage-Gated Sodium Channel †

**ARTICLE** *in* BIOCHEMISTRY · FEBRUARY 2008

Impact Factor: 3.02 · DOI: 10.1021/bi701323k · Source: PubMed



**6 AUTHORS**, INCLUDING:

Roy Kahn
InSight Biopharmaceuticals Ltd.
**22** PUBLICATIONS **501** CITATIONS
SEE PROFILE

Dalia Gordon
Weizmann Institute of Science
**126** PUBLICATIONS **4,154** CITATIONS
SEE PROFILE

# NMR Analysis of Interaction of LqhαIT Scorpion Toxin with a Peptide Corresponding to the D4/S3−S4 Loop of Insect Para Voltage-Gated Sodium Channel†

Einat Schnur,‡ Michael Turkov,§ Roy Kahn,§ Dalia Gordon,§ Michael Gurevitz,§ and Jacob Anglister*,‡

*Department of Structural Biology, Weizmann Institute of Science, Rehovot 76100, Israel, and Department of Plant Sciences, George S. Wise Faculty of Life Sciences, Tel Aviv University, Ramat-Aviv 69978, Tel Aviv, Israel*

*Received July 5, 2007; Revised Manuscript Received November 4, 2007*

ABSTRACT: Voltage-gated sodium channels ($Na_v$s) are large transmembrane proteins that initiate action potential in electrically excitable cells. This central role in the nervous system has made them a primary target for a large number of neurotoxins. Scorpion α-neurotoxins bind to $Na_v$s with high affinity and slow their inactivation, causing a prolonged action potential. Despite the similarity in their mode of action and three-dimensional structure, α-toxins exhibit great variations in selectivity toward insect and mammalian $Na_v$s, suggesting differences in the binding surfaces of the toxins and the channels. The scorpion α-toxin binding site, termed neurotoxin receptor site 3, has been shown to involve the extracellular S3−S4 loop in domain 4 of the α-subunit of voltage-gated sodium channels (D4/S3−S4). In this study, the binding site for peptides corresponding to the D4/S3−S4 loop of the para insect $Na_v$ was mapped on the highly insecticidal α-neurotoxin, LqhαIT, from the scorpion *Leiurus quinquestriatus hebraeus*, by following changes in the toxin amide $^1$H and $^{15}$N chemical shifts upon binding. This analysis suggests that the five-residue turn (residues $^{Lq}$K8−$^{Lq}$C12) of LqhαIT and those residues in its vicinity interact with the D4/S3−S4 loop of $Na_v$. Residues $^{Lq}$R18, $^{Lq}$W38, and $^{Lq}$A39 could also form a patch contributing to the interaction with D4/S3−S4. Moreover, a new bioactive residue, $^{Lq}$V13, was identified as being important for $Na_v$ binding and specifically for the interaction with the D4/S3−S4 loop. The contribution of $^{Lq}$V13 to $Na_V$ binding was further verified by mutagenesis. Future studies involving other extracellular regions of $Na_v$s are required for further characterization of the structure of the LqhαIT−$Na_v$s binding site.

Voltage-gated sodium channels ($Na_v$s)[1] are responsible for the voltage-dependent transient increase in sodium ion permeability, which is critical for action potential initiation and propagation in neurons and most electrically excitable cells (*1*−*3*). The key features of $Na_v$s include efficient and selective conduction of sodium ions and their gating behavior, which is the ability to rapidly activate and inactivate upon cell membrane depolarization (*1*, *3*, *4*). Sodium channel dysfunctions can cause a range of diseases termed "channelopathies" such as generalized epilepsy, hyperkalemic periodic paralysis, and progressive familial heart block (*3*, *5*, *6*).

$Na_v$s are transmembrane proteins composed of a large (∼260 kDa) pore-forming α-subunit associated with auxiliary β-subunits (∼38 kDa) that modify the α-subunit function in a cell-type specific manner (*1*, *7*, *8*). The α-subunit is organized into four repeat domains (D1−D4), each containing six α-helical transmembrane segments (S1−S6), connected by internal and external loops. The S4 segments in each of the four domains are positively charged and function as voltage sensors. It has been suggested that upon membrane depolarization, the S4 segments move toward the extracellular space, imposing a conformational change that leads to channel activation and influx of sodium ions (*2*, *9*, *10*). The outward movement of the S4 segment of the D4 domain (D4/S4) is required for the coupling of channel activation to its inactivation (*9*, *11*). Inactivation is mediated by a short intracellular loop connecting domains D3 and D4 (*1*, *12*). The membrane-reentrant loop between S5 and S6 (SS1−SS2), termed the P-loop, forms the ion selectivity filter and together with the S5 and S6 transmembrane segments lines the walls of the sodium ion-conducting pore (*1*).

Because of their structural conservation and key role in neuronal excitability, $Na_v$s are molecular targets for a variety of neurotoxins that are produced in a wide array of organisms

† This study was supported by NIH Grant NS38301 (J.A.) and by the Kimmelman Center for Biomolecular Structure and Assembly (J.A.); by United States-Israel Binational Agricultural Research and Development Grants IS-3928-06 (M.G. and D.G.) and IS-4066-07 (D.G. and M.G.); by Israeli Science Foundation Grant 909/04 (M.G.); and by NIH Grant 1 U01 NS058039-01 (M.G.). J.A. is the Dr. Joseph and Ruth Owades Professor of Chemistry.

* To whom correspondence should be addressed. E-mail: Jacob.Anglister@weizmann.ac.il. Phone: 972-8-9343394. Fax: 972-8-9344136.

‡ Weizmann Institute of Science.

§ Tel Aviv University.

[1] Abbreviations: NMR, nuclear magnetic resonance; $Na_v$s, voltage-gated sodium channels; D4/S3−S4, extracellular loop connecting segments 3 and 4 in domain 4 of the α-subunit of voltage-gated sodium channels; LqhαIT, *Leiurus quinquestriatus hebraeus* α-insect toxin; HPLC, high-pressure liquid chromatography; HOHAHA, homonuclear Hartman−Hahn spectroscopy; NOESY, nuclear Overhauser effect spectroscopy; HSQC, heteronuclear single-quantum correlation; CSD, chemical shift difference; TFA, trifluoroacetic acid.

10.1021/bi701323k CCC: $40.75 
Published on Web 12/23/2007

(*2*, *13*). At least six neurotoxin receptor sites have been identified on $Na_v$s (*2*, *14*, *15*).

Scorpion toxins are 61−76-residue proteins that modulate the gating properties of voltage-gated $Na_v$s. According to their mode of action and binding properties, scorpion toxins are divided into two major classes, α- and *β*-toxins. Scorpion α-toxins prolong the action potential by inhibiting channel inactivation, possibly through interference with the outward movement of the D4/S4 segment necessary for the fast inactivation process. The binding site of scorpion α-neurotoxins on $Na_v$s is named neurotoxin receptor site 3 (*1*, *14*). It is situated on the pore-forming α-subunit and involves extracellular S5−S6 loops of D1 and D4 (*16*, *17*) and the S3−S4 loop in D4 (D4/S3−S4), as revealed by Catterall and co-workers when they tested the affinity of scorpion α-toxin for $Na_v$s with mutations of extracellular acidic amino acids (*1*, *9*). Scorpion *β*-toxins bind to receptor site 4 assigned to extracellular S1−S2 and S3−S4 loops in D2 of the sodium channel (*1*, *2*, *18*) and shift the activation of the channel to more negative membrane potentials (*1*, *2*, *19*−*21*). Currently, most of the knowledge about the binding site of scorpion α-toxins on $Na_v$s has been gained by channel mutagenesis studies (*2*, *9*, *22*).

Scorpion α-toxins are similar in structure and exhibit a similar mode of action but are very diverse in sequence and selectivity. Some scorpion α-neurotoxins exhibit specificity for insect $Na_v$s, and others are specific for mammalian $Na_v$s and exhibit different affinities for sodium channel subtypes in mammalian neurons (*23*−*25*). On the basis of their selectivity for mammals and insects, scorpion α-toxins were divided into three pharmacological subgroups: (i) classical anti-mammalian toxins that bind with high affinity to rat brain synaptosomes and are practically nontoxic to insects, (ii) α-toxins that are highly active on insects, bind with high affinity to insect $Na_v$s, and are weakly toxic in mammalian brain, and (iii) α-like toxins that are active in both mammalian brain and insects (*15*, *20*).

LqhαIT, a 64-residue highly insecticidal scorpion toxin from *Leiurus quinquestriatus hebraeus* (yellow scorpion) venom, was classified as an α-toxin on the basis of its structural and functional similarities to other scorpion α-toxins (*26*). It is the most insecticidal among scorpion α-toxins. The structure of LqhαIT was determined by NMR and was found to resemble that of other scorpion toxins: a core composed of an α-helix packed against a three-stranded antiparallel *β*-sheet and stabilized by four disulfide bonds (Protein Data Bank entries 1LQH and 1LQI) (*27*).

Previous mutagenesis studies of LqhαIT have identified two clusters of residues important for its binding to $Na_v$s. Mutations $^{Lq}$Y10S/A,[2] $^{Lq}$F17G/W, $^{Lq}$R18A, $^{Lq}$W38A/Y, and $^{Lq}$N44A and of most residues of the C-tail region ($^{Lq}$I57A/T, $^{Lq}$R58K, $^{Lq}$V59A/G, $^{Lq}$R58K/V59A, $^{Lq}$K62A/L/R, and $^{Lq}$R64N) reduced toxin activity considerably (*28*, *29*). The majority of LqhαIT residues found to be important for function are conserved in most scorpion α-toxins. Among them are $^{Lq}$R18, an aromatic residue at position 38, $^{Lq}$N44, and a positively charged residue at position 58 (*28*−*31*). Site-directed mutagenesis and binding assays were also used to investigate the role of the D4/S3−S4 loop in determining the selectivity of the α-toxins toward insect and mammalian $Na_v$s. These studies suggested that toxins of the various subgroups bind differently to neurotoxin receptor site 3 (*24*, *25*). Despite the identification of residues involved in binding, it is not known which regions or residues in scorpion toxins interact with which regions or residues on sodium channels.

Because of their large size and membranal localization, $Na_v$s present a major challenge for both X-ray and NMR studies and their high-resolution structure has not yet been determined (*3*). A structure of the sodium channel at 19 Å resolution was determined by cryo-electron microscopy and single-particle image analysis (*4*, *32*). To overcome the difficulties in NMR studies of complexes of large membrane proteins with soluble ligands, the interaction of these ligands with isolated segments of the membrane protein can be investigated, as we and others have demonstrated in the study of interaction of α-bungarotoxin with the nicotinic acetylcholine receptor (*33*, *34*). Although the free peptide of the cognate membrane proteins was flexible in solution, it adopted a well-defined *β*-hairpin conformation when bound to the toxin.

This study reveals that peptides corresponding in sequence to the D4/S3−S4 loop exhibit millimolar affinity for LqhαIT. Analysis of the perturbations in LqhαIT chemical shifts was used to map the binding site for the S3−S4 loop on the scorpion toxin and provided new insights into receptor site 3 and the toxin binding mechanism.

## EXPERIMENTAL PROCEDURES

*Peptide Synthesis.* The D4/S3−S4 peptides were synthesized on a peptide solid-phase synthesizer (Advanced ChemTech, Louisville, KY). The peptides were purified by reverse-phase HPLC (Thermo Separation Products) on a C4 or C18 preparative column (250 mm × 25 mm; GraceVydac), using the following shallow acetonitrile/water gradients: 18 to 22% acetonitrile over 60 min for RRG($^{NaC}$S$_{1700}$−T$_{1711}$)GRR, 21 to 24% acetonitrile over 60 min for the peptides DDG($^{NaC}$S$_{1700}$−T$_{1711}$)GDD and SSG($^{NaC}$S$_{1700}$−T$_{1711}$)-GSS, and 43 to 45% acetonitrile over 60 min for SS($^{NaC}$S$_{1693}$−T$_{1711}$)GSS. All solvents contained 0.1% trifluoroacetic acid (TFA). Purity and molecular weight were confirmed by electrospray mass spectrometry. Cholera toxin peptide 3, CTP3 (CH$_3$CO-VEVPGSQHIDSQKKAA-NH$_2$), was synthesized and purified as previously described (*35*).

*Peptide Expression.* To enable future $^{15}$N labeling of the D4/S3−S4 peptides, we developed an expression system for the peptide RRR($^{NaC-1693}$SILGLVLSDIIEKYFVSPTLLR$^{1714}$)-RR. Since peptides are usually not overexpressed well in bacteria, as they are degraded inside the cell, the peptide was expressed in fusion with a TrpΔLE carrier protein (*36*). The coding DNA for a peptide corresponding to the D4/S3−S4 loop (residues 1693−1713) of *Drosophila melanogaster* sodium channel DmNa$_v$1, including two TAA stop codons, was linked to the TrpΔLE polypeptide sequence using *Hin*dIII and *Bam*HI restriction sites in the pET24a vector. A triple hydroxylamine cleavage site, Asn-Gly (*37*), was inserted using a QuikChange XL site-directed mutagenesis kit (Stratagene, La Jolla, CA). The expressed fusion protein His$^{Tag}$-TrpΔLE-NGNGNGRRRSILGLVLSDIIEKY-FVSPTLLRRR contains the entire D4/S3−S4 loop as well as the second helix of S3 which may be only partially buried

[2] Sodium channel and LqhαIT residues are marked by NaC and Lq superscripts, respectively.

in the cell membrane (*38*, *39*). Residue $^{NaC}R_{1714}$ is the beginning of the transmembranal S4 domain. Three and two arginine residues were added at the N- and C-termini of the peptide, respectively, to ensure solubility, since it contains many hydrophobic residues. Transformed *Escherichia coli* Rosetta DE3 cells were grown in LB. Expression was induced with 1 mM isopropyl β-D-thiogalactopyranoside (IPTG) (Fermentas) when the culture reached an optical density of approximately 0.7 at 595 nm. Expression was continued overnight at 310 K with constant shaking at 225 rpm. Cells were harvested by centrifugation (8000 rpm for 30 min), suspended in washing buffer [50 mM Tris (pH 7.8), 0.5 mM EDTA, 50 mM NaCl, and 5% glycerol], and sonicated for 100 s. The 16 kDa overexpressed fusion protein was sequestered in inclusion bodies. The cell lysate was centrifuged at 12 000 rpm for 15 min at 277 K, and the pellet containing the inclusion bodies was washed three times with the washing buffer. The inclusion bodies were suspended in 6 M guanidine-HCl, 1 M hydroxylamine-HCl, and 50 mM free methionine (pH 9) at 318 K for 4.5 h. The peptide was cleaved from the TrpΔLE carrier protein by hydroxylamine (*37*). The cleavage was terminated by the addition of formic acid to pH 7. The cleaved peptide was purified by reverse-phase HPLC (Thermo Separation Products) on a preparative C4 reverse-phase column (250 mm × 25 mm; GraceVydac), using an acetonitrile/water gradient of 40 to 47% acetonitrile over 60 min. All solvents contained 0.1% trifluoroacetic acid (TFA). Purity and molecular weight were confirmed by electrospray mass spectrometry.

*Expression of $^{15}$N-Labeled Toxin*. *E. coli* strain BL21 carrying a pET11cK vector bearing the cDNA encoding LqhαIT was used for toxin expression (*40*). Cells were grown in M9 minimal medium with $^{15}NH_4Cl$ (98% $^{15}$N, Sigma-Aldrich, St. Louis, MO) containing 40 μg/mL kanamycin and 30 μg/mL chloramphenicol. The inducer IPTG (BioLab) was added at an $OD_{600}$ of 0.5 to a final concentration of 0.4 mM and the growth continued for an additional 20 h. Cells from 1 L of culture were harvested by centrifugation, resuspended in 50 mL of water, and lysed by being frozen and thawed. The cell lysate was sonicated on ice, and the insoluble pellet fraction (22000 *g* for 15 min) was washed with buffer [25% (w/v) sucrose, 5 mM EDTA, and 1% (v/v) Triton X-100 in PBS]. The toxin was folded following denaturation and renaturation as previously described (*31*). A 3 mL Resource column (Amersham) was employed for $^{15}$N toxin purification by reverse-phase HPLC using a three-step gradient of acetonitrile (0 to 25%, 25 to 31%, and 31 to 100%) and 0.1% (v/v) trifluoroacetic acid (TFA) in water. The eluted solution was dialyzed against water and was concentrated by ultrafiltration (Vivaspin20, Sartorius) to 10 mg/mL (1.5 mM). Site-directed mutagenesis was performed by PCR, as described previously (*29*).

*Toxicity Assays.* Four-day-old blowfly larvae (*Sarcophaga falculata*; 150 ± 20 mg of body weight) were injected intersegmentally. A positive result was scored when a characteristic paralysis (immobilization and contraction) was observed up to 5 min after injection. Five concentrations of each toxin were injected into larvae (nine larvae in each group) in three independent experiments. The 50% effective dose ($ED_{50}$) values were calculated as described previously (*29*).

*Electrophysiological Assays.* cRNAs encoding the *D. melanogaster* para ($DmNa_v1$) sodium channel α-subunit and the auxiliary β-subunit TipE were transcribed in vitro and injected into *Xenopus laevis* oocytes as described previously (*41*). Currents were measured 1−4 days after injection using the two-electrode voltage clamp technique described previously (*42*). The bath solution contained 96 mM NaCl, 2 mM KCl, 1 mM $MgCl_2$, 2 mM $CaCl_2$, and 5 mM HEPES (pH 7.85). The toxins were diluted with bath solution containing 1 mg/mL BSA and applied directly to the bath to the final desired concentration. Currents were elicited by depolarization to −10 mV from a holding potential of −80 mV in the presence of several toxin concentrations. The dose-dependent effect of the toxin (removal of fast inactivation) was calculated by plotting the ratio of the steady-state current measured 50 ms after depolarization ($I_{ss}$) to the peak current ($I_{peak}$) as a function of toxin concentration and fitting with the Hill equation $I_{ss}/I_{peak} = a_0 + (a_1 - a_0)/(1 + EC_{50}/[toxin])^H$, where $H$ is the Hill coefficient, [toxin] is the toxin concentration, and $a_0$ is the offset measured prior to toxin application. The amplitude $a_1 - a_0$ provides the maximal effect obtained at saturating toxin concentrations. $EC_{50}$ is the toxin concentration that causes half-maximal inhibition of fast inactivation. To minimize variability, $H$ was set to 1 in all calculations.

*NMR Sample Preparation.* All NMR samples, except for the one used for RRG($^{NaC}S_{1700}$−$T_{1711}$)GRR titration, were dissolved in 350 μL of a 95% $H_2O$/5% $D_2O$ mixture, containing 10 mM phosphate buffer and 0.05% $NaN_3$. Samples of uniformly labeled [$^{15}$N]LqhαIT ([U-$^{15}$N]LqhαIT) and peptides were prepared at the same pH, either pH 5.2 or 7.0. The sample for LqhαIT $^{15}$N and amide proton chemical shift assignments contained 0.9 mM toxin. For the titration of [U-$^{15}$N]LqhαIT with RRG($^{NaC}S_{1700}$−$T_{1711}$)GRR, a 5.0 mM solution of the peptide was prepared and added stepwise into a sample of 0.24 mM [U-$^{15}$N]LqhαIT, until a 7:1 peptide:toxin molar ratio was reached (the [U-$^{15}$N]-LqhαIT concentration at the end of titration was 0.18 mM; the maximum peptide concentration was 1.28 mM). For the titration of [U-$^{15}$N]LqhαIT with DDG($^{NaC}S_{1700}$−$T_{1711}$)GDD, a 5.9 mM solution of the peptide was prepared and added stepwise into a sample of 0.15 mM [U-$^{15}$N]LqhαIT, until a 10.5:1 peptide:toxin molar ratio was reached (the [U-$^{15}$N]-LqhαIT concentration at the end of titration was 0.12 mM; the maximum peptide concentration was 1.26 mM). For the titration of [U-$^{15}$N]LqhαIT with SSG($^{NaC}S_{1700}$−$T_{1711}$)GSS, a 7.0 mM solution of the peptide was prepared and added stepwise into a sample of 0.20 mM [U-$^{15}$N]LqhαIT, until a 15:1 peptide:toxin molar ratio was reached (the [U-$^{15}$N]-LqhαIT concentration at the end of titration was 0.14 mM; the maximum peptide concentration was 2.14 mM). Because of the poor solubility of the elongated peptide, SS($^{NaC}S_{1693}$−$T_{1711}$)GSS, the toxin solution was added to lyophilized peptide to yield the maximum concentration of the peptide. The SS($^{NaC}S_{1693}$−$T_{1711}$)GSS:toxin ratio in the NMR sample was 7:1. The final concentrations of toxin and peptide in the sample were 0.08 and 0.6 mM, respectively. Concentrations were determined using UV absorbance measurement at 280 nm. For the titration of [U-$^{15}$N]LqhαIT with CTP3, a 10.0 mM solution of the peptide was prepared and added stepwise into a sample of 0.15 mM [U-$^{15}$N]LqhαIT, until an 8:1 peptide:toxin molar ratio was reached (the [U-$^{15}$N]-

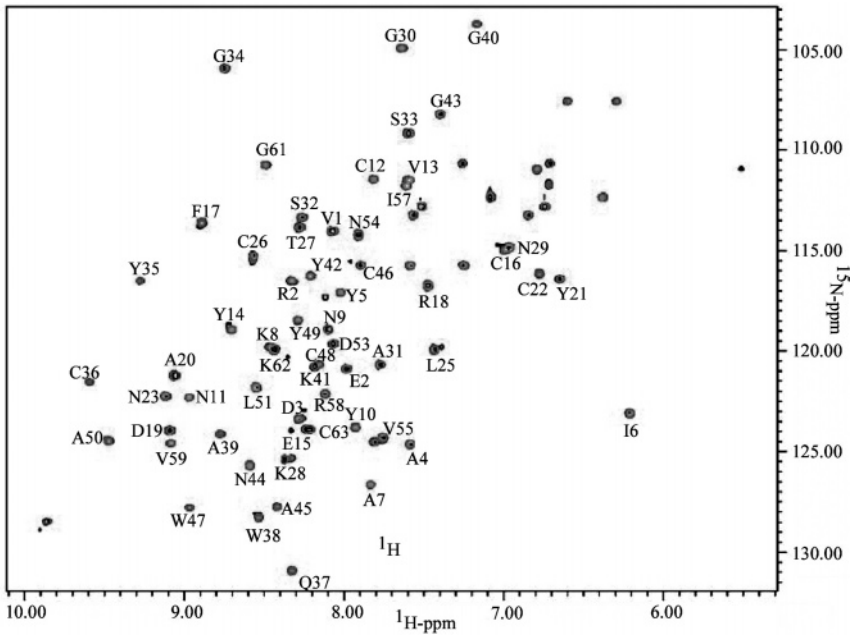


FIGURE 1: $^{1}H-^{15}N$ HSQC spectrum of [U-$^{15}N$]LqhαIT. $^{1}H-^{15}N$ HSQC spectrum of 0.9 mM LqhαIT uniformly labeled with $^{15}N$ acquired at 293 K and pH 5.2 on an 800 MHz NMR spectrometer. The backbone amide assignment is shown.

LqhαIT concentration at the end of titration was 0.13 mM; the maximum peptide concentration was 1.02 mM).

The NMR sample for RRR($^{NaC}S_{1693}-R_{1714}$)RR titration was dissolved in 350 $\mu$L of a 95% $H_2O$/5% $D_2O$ mixture, containing 10 mM deuterated acetate buffer (pH 4.8) and 0.005% thimerosal. For the titration of [U-$^{15}N$]LqhαIT with RRG($^{NaC}S_{1700}-T_{1711}$)GRR, a 7.8 mM solution of the peptide was prepared and added stepwise to a sample of 0.20 mM [U-$^{15}N$]LqhαIT, until a 9:1 peptide:toxin molar ratio was reached (the [U-$^{15}N$]LqhαIT concentration at the end of titration was 0.16 mM; the maximum peptide concentration was 1.45 mM).

*NMR Measurements.* All NMR spectra were measured on a Bruker DRX 800 MHz spectrometer. Two-dimensional (2D) HOHAHA and NOESY spectra of the peptides were acquired at 277 K using mixing times of 200 and 100 ms, respectively. Three-dimensional (3D) $^{15}N$-separated HOHAHA and NOESY spectra of [U-$^{15}N$]LqhαIT were recorded at 293 K using mixing times of 70 and 200 ms, respectively. $^{1}H-^{15}N$ HSQC spectra were acquired at 277, 285, and 293 K. Data were processed and analyzed using XWIN-NMR, NMRPipe (*43*), and NMRView (*44*, *45*).

*Dissociation Constant Evaluation.* Dissociation constants ($K_d$) of the toxin−peptide complexes were evaluated from $^{1}H-^{15}N$ HSQC titration experiments and were used as means to assess the binding of the different peptides relative to one another. LqhαIT chemical shift differences (CSDs) were calculated by $[\Delta(\delta H)^2 + \Delta(\delta N/5)^2]^{1/2}$, where $\Delta(\delta H)$ and $\Delta(\delta N)$ are the changes in $^{1}H$ and $^{15}N$ chemical shifts, respectively (*46*). Data of LqhαIT CSD as a function of added peptide concentration were fitted to a 1:1 simple binding model, by a nonlinear square fit, using ORIGIN version 7.5 (OriginLab Corp.). Minimal $K_d$ values were calculated from the chemical shift changes of $^{Lq}$V13 of LqhαIT, which is the backbone residue that exhibited the largest CSD.

## RESULTS

*$^{15}N$ Chemical Shift Assignment of LqhαIT.* Chemical shifts are very sensitive to variations in the local electronic environment. The $^{1}H-^{15}N$ HSQC spectrum of proteins enables monitoring the changes in chemical shifts upon binding, in a residue specific manner, and can be used to map the binding determinants of proteins and their ligands (*46*−*48*).

The $^{1}H-^{15}N$ HSQC spectrum of uniformly labeled [$^{15}N$]-LqhαIT ([U-$^{15}N$]LqhαIT) is very well resolved as shown in Figure 1. All backbone non-proline amide chemical shifts of [U-$^{15}N$]LqhαIT, except for the N-terminal methionine, were assigned using 3D $^{15}N$-separated HOHAHA and 3D $^{15}N$-separated NOESY spectra and standard procedures. The amine proton of the N-terminal methionine was not detected due to fast exchange with water. All side chain $^{15}N$ chemical shifts, except for the side chain $N_\varphi$ of lysine and $N_{\eta 1}$ and $N_{\eta 2}$ of arginine residues, were assigned as well (Figure 1). The side chain $\varphi$ protons of lysine and $\eta_1$ and $\eta_2$ protons of arginine residues were not detected probably since they are outside the $^{15}N$ chemical shift range detected in the measured $^{1}H-^{15}N$ HSQC spectra that show the backbone and side chain amide $^{1}H-^{15}N$ cross-peaks.

*Binding of D4/S3*−*S4 Peptides to LqhαIT.* The D4/S3−S4 loop has been implicated in α-scorpion toxin binding (*9*). To map the LqhαIT surface interacting with D4/S3−S4, we synthesized peptides corresponding in sequence to this loop (Table 1), used them to titrate the uniformly $^{15}N$-labeled toxin, and followed the changes in chemical shifts of the toxin's $^{1}H-^{15}N$ cross-peaks upon peptide binding. Since the structure of LqhαIT is compact and very rigid (*27*), no major conformational changes are expected upon binding to the flexible channel peptides, and changes in chemical shifts are expected to be localized to residues involved in binding. As shown later, the majority of resonances are indeed not affected by the addition of the titrated peptides.

Table 1: Sequences and Molecular Weights of Sodium Channel Peptides Used for LqhαIT Binding Studies[a]

| Peptide Name | Sequence | Molecular Weight (gr/mol) |
|---|---|---|
| $^{NaC}$D4/S3-S4 loop | $^{1691}$ILSILGLVLSDIIEKYFVSPTLLRVVR$^{1717}$ | |
| RRG($^{NaC}$S$_{1700}$-T$_{1711}$)GRR | RRG**SDIIEKYFVSPT**GRR | 2137.4 |
| DDG($^{NaC}$S$_{1700}$-T$_{1711}$)GDD | DDG**SDIIEKYFVSPT**GDD | 1973.0 |
| SSG($^{NaC}$S$_{1700}$-T$_{1711}$)GSS | SSG**SDIIEKYFVSPT**GSS | 1860.9 |
| SS($^{NaC}$S$_{1693}$-T$_{1711}$)GSS | SS**SILGLVLSDIIEKYFVSPT**GSS | 2499.8 |
| RRR($^{NaC}$S$_{1693}$-R$_{1714}$)RR | RRR**SILGLVLSDIIEKYFVSPTLLR**RR | 3257.9 |

[a] Underlined residues of the S3−S4 loop are part of the hypothetical transmembrane segments. Residues highlighted in bold are from the S3−S4 loop sequence.

The dissociation constant of LqhαIT from insect Na$_v$s is in the nanomolar range (*15*). Since the D4/S3−S4 extracellular loop is most likely only a part of neurotoxin receptor site 3 (*17*−*19*), considerably weaker binding is expected for the D4/S3−S4 peptides. To enable measurements of binding up to a dissociation constant of 1 mM, the D4/S3−S4 peptide should be soluble in the 1−5 mM range. To achieve such high solubility, we initially synthesized short peptides that consisted of the D4/S3−S4 extracellular loop without its flanking hydrophobic segments. To increase the solubility of the D4/S3−S4 peptide, $^{NaC}$SDILEKYFVSPT, corresponding to residues 1700−1711 of DmNa$_v$1, solubility tags were added to the N- and C-termini of the peptide.

Initially, we added two arginines and a glycine at each terminus of the peptide RRGSDIIEKYFVSPTGRR [RRG($^{NaC}$S$_{1700}$−T$_{1711}$)GRR] to increase its solubility. The $^1$H−$^{15}$N HSQC spectra of the free [U-$^{15}$N]LqhαIT toxin and of [U-$^{15}$N]LqhαIT at increasing concentrations of RRG($^{NaC}$S$_{1700}$−T$_{1711}$)GRR peptide were recorded, and the changes in the $^1$H−$^{15}$N cross-peaks of the toxin as a function of the added peptide concentration were examined. Most of the toxin's $^1$H−$^{15}$N HSQC cross-peaks did not change their chemical shifts, even at 1.28 mM peptide (7-fold excess with respect to the toxin concentration), while other cross-peaks gradually shifted as the peptide:toxin ratio in the sample increased. This concentration-dependent movement of the cross-peaks upon addition of peptide indicates binding (Figure 2A). Backbone $^1$H−$^{15}$N cross-peaks of two residues, namely, $^{Lq}$K8 and $^{Lq}$V13, exhibited significant chemical shift changes (>0.03 ppm) upon binding to the peptide (0.035 ppm for $^{Lq}$K8 and 0.065 ppm for $^{Lq}$V13), suggesting that these two residues are involved in binding. In addition, the $^1$H−$^{15}$N$\epsilon$ cross-peak of $^{Lq}$R58 also shifted significantly (0.090 ppm).

Under conditions of fast exchange usually associated with weak binding, a single peak at the weighted average chemical shifts of the free and bound forms is observed, whereas in slow exchange, separate signals are observed for the free and bound forms (*47*, *48*). As seen from the gradual changes in chemical shift during the titration of the toxin with the DmNa$_v$1-derived peptide and the appearance of a single cross-peak, the kinetics of binding of LqhαIT to RRG($^{NaC}$S$_{1700}$−T$_{1711}$)GRR is in the fast exchange regime.

*Evaluation of the Dissociation Constant.* The dependence of the changes in chemical shift on the concentration of the added peptide provides a convenient indirect measure of the complex concentration and therefore can be used to determine its dissociation constant. The changes in chemical shift as a function of the added peptide concentration were plotted, and a global fit to a 1:1 simple binding model [CSD = $\Delta(\delta^{max}) \times x/(K_d + x)$] was calculated. The peptide RRG($^{NaC}$S$_{1700}$−T$_{1711}$)GRR exhibited a $K_d$ of 0.9 ± 0.4 mM (Figure 3), corresponding approximately to one-third of the binding free energy, $\Delta G$, of the sodium channel with the scorpion toxin.

*Optimization of Conditions for Comparison of the Different DmNa$_v$1 Peptides.* To determine the temperature at which largest deviations in chemical shift between the free toxin and the toxin bound to the D4/S3−S4 peptides are observed, $^1$H−$^{15}$N HSQC spectra of the free toxin and the toxin in the presence of a 7-fold excess of RRG($^{NaC}$S$_{1700}$−T$_{1711}$)GRR (the sample obtained after the titration described above) were measured at 293, 285, and 277 K. The observed deviations in chemical shift increased as the temperature decreased (0.037 ppm at 293 K, 0.049 ppm at 285 K, and 0.065 ppm at 277 K for $^{Lq}$V13), suggesting tighter binding at lower temperatures.

To determine the optimal pH for following CSDs upon peptide binding, samples were prepared at pH 5.2 and 7.0. No significant changes in complex formation were detected between the two conditions, as determined by comparison of the CSDs upon peptide binding. The binding of LqhαIT to sodium channels in insect neuronal membranes was also not affected by pH changes in the range between 5.5 and 8.5 (*31*, *49*). Therefore, to represent a more physiological pH, all samples were prepared thereafter at pH 7.0, and all NMR spectra were collected at 277 K.

*Binding of Peptides with Negatively Charged or Neutral Solubility Tags.* To examine whether the positive charges contribute to the binding of the peptide RRG($^{NaC}$S$_{1700}$−T$_{1711}$)-GRR to LqhαIT, additional titration experiments were conducted with the peptides DDG($^{NaC}$S$_{1700}$−T$_{1711}$)GDD and SSG($^{NaC}$S$_{1700}$−T$_{1711}$)GSS that have extra negative charges or neutral hydrophilic residues at their termini. The $^1$H−$^{15}$N HSQC cross-peaks of $^{Lq}$K8, $^{Lq}$V13, and $^{Lq}$R58 N$\epsilon$, which shifted upon binding of RRG($^{NaC}$S$_{1700}$−T$_{1711}$)GRR to LqhαIT, exhibited similar changes in chemical shifts upon the addition of DDG($^{NaC}$S$_{1700}$−T$_{1711}$)GDD (0.082 ppm for $^{Lq}$K8, 0.078 ppm for $^{Lq}$V13, and 0.100 ppm for $^{Lq}$R58 upon addition of 1.26 mM peptide) or SSG($^{NaC}$S$_{1700}$−T$_{1711}$)GSS (0.039 ppm for $^{Lq}$K8, 0.083 ppm for $^{Lq}$V13, and 0.113 ppm for $^{Lq}$R58 upon addition of 2.14 mM peptide) (Figure 4), indicating that the solubility tags have very little effect on the binding of D4/S3−S4-derived peptides ($^{NaC}$S$_{1700}$−T$_{1711}$) to LqhαIT. In addition, $^{Lq}$R18 and $^{Lq}$Q37 exhibited changes in chemical shifts above the background level for both DDG($^{NaC}$S$_{1700}$−T$_{1711}$)GDD and SSG($^{NaC}$S$_{1700}$−T$_{1711}$)GSS (0.099 and 0.041 ppm for $^{Lq}$R18, respectively, and 0.035 and 0.031 ppm for $^{Lq}$Q37, respectively) (Figure 4). Interestingly, the background levels of changes in CSD values upon titration with DDG($^{NaC}$S$_{1700}$−T$_{1711}$)GDD were slightly higher than those observed for the other two peptides, suggesting possible minute perturbation due to nonspecific interactions caused by the addition of the negatively charged solubility tags at the sodium channel peptide termini. LqhαIT has a net of three positive charges, which could account for this observation. Furthermore, the toxin region that is especially rich in positive charges is the C-terminal tail, which was suggested to contribute to the toxin binding to the sodium channel (*23*, *29*, *50*). The changes in [U-$^{15}$N]LqhαIT chemical shifts upon

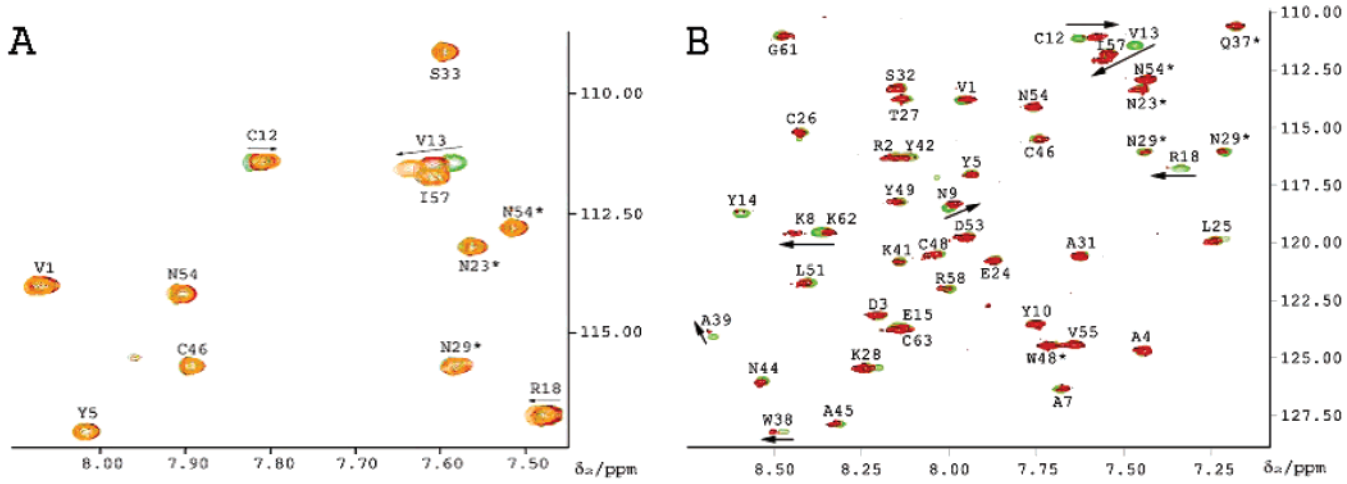


FIGURE 2: Overlay of $^{1}H-^{15}N$ HSQC spectra of [U-$^{15}$N]LqhαIT titrated with D4/S3−S4 peptides. (A) Spectra of [U-$^{15}$N]LqhαIT alone (green), [U-$^{15}$N]LqhαIT and RRG($^{NaC}S_{1700}-T_{1711}$)GRR in a 1:2 molar ratio (red), and [U-$^{15}$N]LqhαIT and RRG($^{NaC}S_{1700}-T_{1711}$)GRR in 1:7 molar ratio (orange). Spectra were collected while titrating with RRG($^{NaC}S_{1700}-T_{1711}$)GRR, at 293 K and pH 5.2. (B) Spectra of [U-$^{15}$N]-LqhαIT alone (green) and [U-$^{15}$N]LqhαIT and SS($^{NaC}S_{1693}-T_{1711}$)GSS in a 1:7 molar ratio (red). Spectra were collected at 277 K and pH 7.0. The depicted spectral regions highlight movement of peaks indicated by arrows, as in the case of $^{Lq}$V13 and $^{Lq}$C12, compared to other peaks that did not change their position. Asterisks mark peaks originating from side chains.

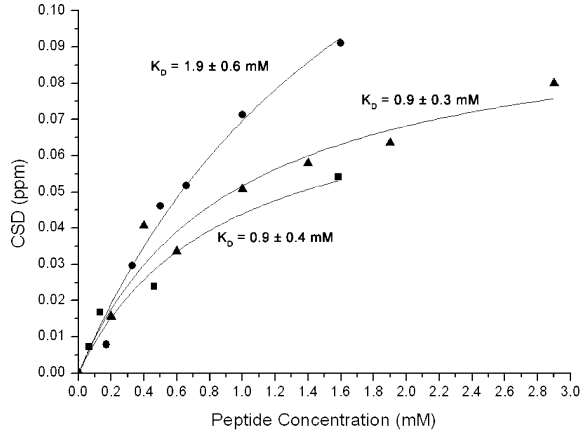


FIGURE 3: Chemical shift changes of $^{Lq}$V13 of LqhαIT as a function of added D4/S3−S4 peptide concentration. Chemical shift deviations (CSDs) of $^{Lq}$V13 as a function of the added concentration of RRG($^{NaC}S_{1700}-L_{1711}$)GRR (■), DDG($^{NaC}S_{1700}-T_{1711}$)GDD (●), and SSG($^{NaC}S_{1700}-T_{1711}$)GSS (▲). Data for RRG($^{NaC}S_{1700}-L_{1711}$)GRR were collected at 293 K. Data for the other two peptides were collected at 277 K. CSD values were calculated using the formula $[\Delta(\delta H)^2 + \Delta(\delta N/5)^2]^{1/2}$, where $\Delta(\delta H)$ and $\Delta(\delta N)$ are the changes in $^{1}$H and $^{15}$N chemical shifts, respectively. The dissociation constant of the peptide−toxin complexes was determined by a nonlinear least-squares fit to the changes in chemical shift as a function of the added peptide concentration.

titration with DDG($^{NaC}S_{1700}-T_{1711}$)GDD or SSG($^{NaC}S_{1700}-T_{1711}$)GSS were used to determine the dissociation constants ($K_d$) for these peptides (Figure 3). The determined $K_d$ values were 1.9 ± 0.6 and 0.9 ± 0.3 mM for DDG($^{NaC}S_{1700}-T_{1711}$)-GDD and SSG($^{NaC}S_{1700}-T_{1711}$)GSS, respectively (Figure 3), indicating that nonspecific binding due to the addition of the negative solubility tags on DDG($^{NaC}S_{1700}-T_{1711}$)GDD was negligible.

*Binding of an Extended D4/S3−S4-Derived Peptide*. In an attempt to increase the affinity of the D4/S3−S4-derived peptide for LqhαIT, we synthesized the peptide SS($^{NaC}S_{1693}-T_{1711}$)GSS. This D4/S3−S4-derived peptide was elongated at its N-terminus by seven residues of the $Na_V$ S3 region ($^{NaC-1693}$SILGLVL$^{1699}$), which might be partially exposed to the solvent (*38*, *39*) (Table 1). Two serine residues were added at each terminus of the peptide to improve its solubility. Neutral polar residues were chosen to exclude any nonspecific interactions of charged residues with the toxin. More than 85% of [U-$^{15}$N]LqhαIT resonances did not change their chemical shifts upon binding of the SS($^{NaC}S_{1693}-T_{1711}$)-GSS peptide, and only less than 15% of the toxin residues did undergo a notable change in chemical shift. Residues $^{Lq}$K8, $^{Lq}$V13, and $^{Lq}$R58 of LqhαIT were found to be involved in binding also with this fourth peptide [0.083, 0.156, and 0.179 ppm changes in LqhαIT chemical shift, respectively, upon addition of 0.6 mM SS($^{NaC}S_{1693}-T_{1711}$)GSS] (Figures 2B and 4).

Five more residues, namely, $^{Lq}$N9, $^{Lq}$C12, $^{Lq}$R18, $^{Lq}$W38, and $^{Lq}$A39, exhibited a more than 0.03 ppm change in chemical shift (0.040 ppm for $^{Lq}$N9, 0.043 ppm for $^{Lq}$C12, 0.031 ppm for $^{Lq}$R18, 0.032 ppm for $^{Lq}$W38, and 0.049 ppm for $^{Lq}$A39), while most residues exhibited a less than 0.015 ppm change. Addition of SS($^{NaC}S_{1693}-T_{1711}$)GSS also resulted in an intensity decrease of some cross-peaks, which was not observed for the three shorter peptides (Figure 5). Intensity loss was pronounced for residues $^{Lq}$Y14, $^{Lq}$R18, $^{Lq}$D19, and especially $^{Lq}$F17, which disappeared completely.

Titration experiments were not carried out for SS($^{NaC}S_{1693}-T_{1711}$)GSS because of its poor solubility in comparison with that of the shorter D4/S3−S4 peptides. Nonetheless, we can estimate that SS($^{NaC}S_{1693}-T_{1711}$)GSS binds LqhαIT tighter than the three shorter peptides since addition of this peptide at a smaller concentration (0.6 mM vs 1.28, 1.26, 2.14, and 1.45 mM for the other D4/S3−S4 peptides) resulted in the largest changes in [U-$^{15}$N]LqhαIT chemical shifts. Moreover, more toxin residues exhibited changes in chemical shift higher than the 0.03 ppm threshold upon binding of the longer sodium channel peptide.

To increase the solubility of the longer D4/S3−S4-derived peptide for determination of the dissociation constant, we replaced the serine solubility tag with an RRR tag. We also added three more residues to the C-terminus to examine whether they contribute additionally to binding. The expressed peptide RRR($^{NaC}S_{1693}$-$R_{1714}$)RR, which was elongated by seven residues at the N-terminus and three residues at

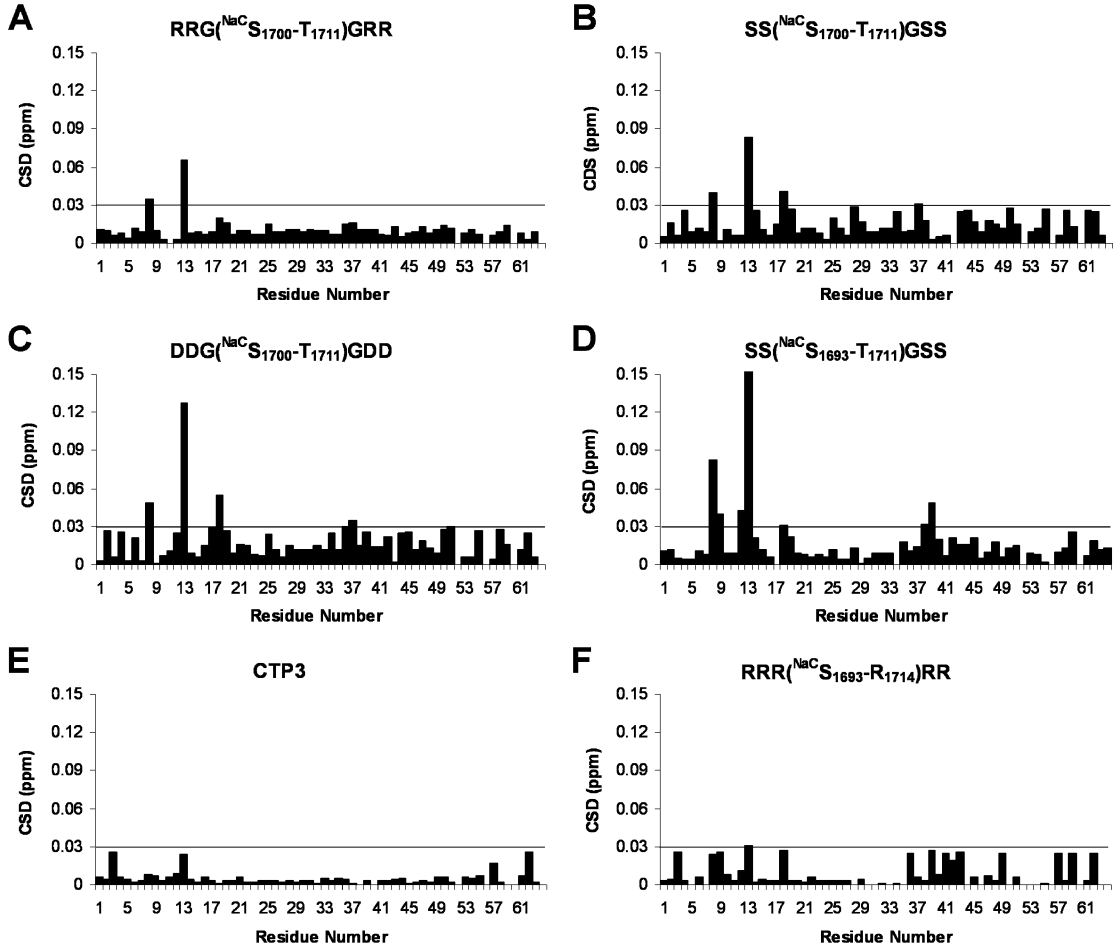


FIGURE 4: Chemical shift deviations of $^{1}H-^{15}N$ LqhαIT cross-peaks induced by binding of D4/S3−S4 peptides or CTP3. Comparison of the chemical shift deviations of $^{1}H-^{15}N$ LqhαIT cross-peaks (CSD) in the $^{1}H-^{15}N$ HSQC spectra upon addition of the different peptides as a function of residue number: (A) RRG($^{NaC}S_{1700}-L_{1711}$)GRR, (B) SSG($^{NaC}S_{1700}-T_{1711}$)GSS, (C) DDG($^{NaC}S_{1700}-T_{1711}$)GDD, (D) SS-($^{NaC}S_{1693}-T_{1711}$)GSS, (E) CTP3, and (F) RRR($^{NaC}S_{1693}-R_{1714}$)RR. CSD values were calculated using the formula $[\Delta(\delta H)^2 + \Delta(\delta N/5)^2]^{1/2}$, where $\Delta(\delta H)$ and $\Delta(\delta N)$ are the changes in $^{1}H$ and $^{15}N$ chemical shifts, respectively. Missing values indicate $^{Lq}$M0, which was not assigned, proline residues, and a few other residues which could not be unambiguously assigned. The 0.03 ppm cutoff is marked.

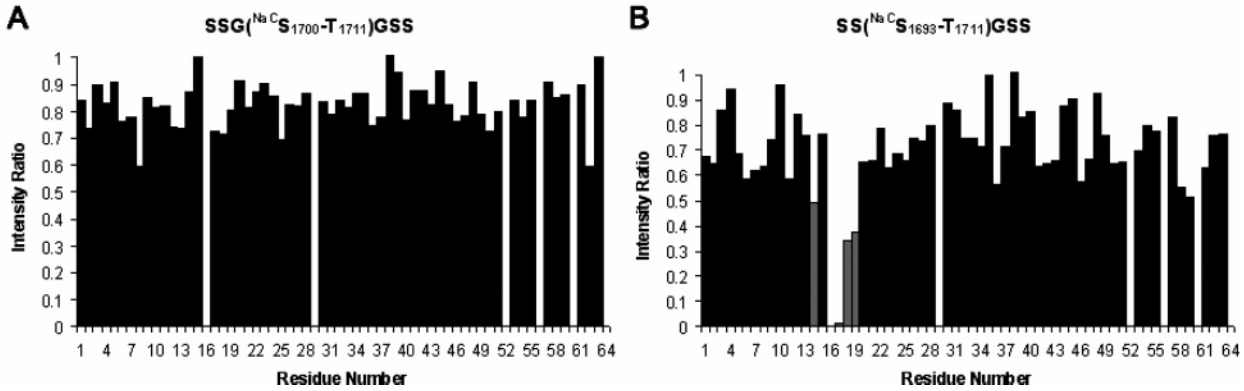


FIGURE 5: Intensity ratio of $^{1}H-^{15}N$ LqhαIT cross-peaks induced by D4/S3−S4 peptide binding. Ratio between cross-peak intensities at the end of the titration and before addition of different D4/S3−S4 peptides as a function of residue number. Missing values indicate $^{Lq}$M0, which was not assigned, $^{Lq}$E16, and $^{Lq}$N29, for which intensities could not be measured due to overlap and proline residues. Gray bars denote residues for which the intensity difference was the largest.

the C-terminus, in comparison with the three shortest peptides, encompasses the entire D4/S3−S4 extracellular loop of $DmNa_v1$. Unlike previous measurements using the shorter channel-derived peptides, titration with RRR($^{NaC}S_{1693}-R_{1714}$)RR resulted in changes in the chemical shift between 0.02 and 0.03 ppm for a large number of LqhαIT residues. Moreover, $^{Lq}$K8, $^{Lq}$V13, and $^{Lq}$R58 also exhibited chemical shift changes in this range, unlike the considerably larger and specific changes observed with the shorter peptides. Since none of LqhαIT residues exhibited a noticeable change in chemical shift upon the addition of RRR($^{NaC}S_{1693}-R_{1714}$)-RR, we conclude that this peptide's binding is too weak to be measured.

*Binding Experiment with an Unrelated Peptide.* To further test our binding results for the D4/S3−S4 peptides, we performed a HSQC titration experiment with an irrelevant

cholera toxin peptide 3 (CTP3) corresponding in sequence to residues 50−64 of the B subunit of cholera toxin ($CH_3$-CO-VEVPGSQHIDSQKKAA-$NH_2$). Titration of [U-$^{15}$N]-LqhαIT with CTP3 resulted in very small chemical shift changes, all beneath the 0.03 ppm cutoff (Figure 4E).

*Mutagenesis of $^{Lq}$V13.* Since $^{Lq}$V13 was found to interact with all the D4/S3−S4-derived peptides and was not examined in previous site-directed mutagenesis studies (*28*, *29*), we analyzed its role in the bioactive surface of LqhαIT by site-directed mutagenesis. Shortening or elongating the side chain of the residue at position 13 by substitutions to alanine or isoleucine ($^{Lq}$V13A and $^{Lq}$V13I, respectively) markedly decreased the toxicity to blowfly larvae (6.1- and 8.3-fold, respectively), and substitution with threonine ($^{Lq}$V13T) decreased the toxicity 16-fold. Electrophysiological studies confirm the bioactive role of this residue (Figure 1 of the Supporting Information). We compared the dose-dependent removal of fast inactivation of the *D. melanogaster* sodium channel DmNa$_v$1 in the presence of LqhαIT and mutants. While LqhαIT is highly potent ($EC_{50} = 0.035 \pm 0.001$ nM; $n = 5$), the $EC_{50}$ values of $^{Lq}$V13A, $^{Lq}$V13I, and $^{Lq}$V13T were 9.0, 5.5, and 335 nM, respectively. These data indicate that $^{Lq}$V13 participates in LqhαIT binding.

## DISCUSSION

*D4/S3−S4 Peptides Bind Specifically to LqhαIT.* NMR is probably one of the best methods for detecting weak binding between two proteins or between proteins and peptides, and it can be used to detect dissociation constants up to 1 mM. In addition, NMR can be used to map the binding surfaces on the proteins. In this study, we have shown that Na$_V$ D4/S3−S4 peptides bind to LqhαIT with a $K_d$ of approximately 1 mM. The use of different solubility tags has eliminated the possibility that these tags influence the binding. Nevertheless, excessive positive charges at the N- and C-termini abolish binding, as demonstrated for the peptide RRR($^{NaC-1693}$SILGLVLSDIIEKYFVSPTLLR$^{1714}$)RR. Addition of this peptide to a concentration of up to 1.45 mM resulted in changes in chemical shifts beneath the 0.03 ppm threshold, and these small changes were observed for a large number of residues. The repulsion between the highly positively charged peptide (net of five positive charges) and the positively charged toxin (a net of three positive charges) is probably responsible for the abolishment of the binding. The practically nondetectable specific binding of RRR-($^{NaC-1693}$SILGLVLSDIIEKYFVSPTLLR$^{1714}$)RR to LqhαIT despite the fact that it contains the D4/S3−S4 sequence supports our conclusion that for the other D4/S3−S4 peptides the binding is specific. Moreover, addition of irrelevant cholera toxin peptide 3 (CTP3) to a concentration of up to 1.04 mM resulted in no CSDs above the 0.03 ppm threshold for any of LqhαIT residues.

Three major regions have been implicated in scorpion α-toxin binding and in the formation of neurotoxin receptor site 3, and these are the D1/S5−S6, D4/S5−D6, and D4/S3−S4 extracellular loops (*9*, *17*). There is no conclusive evidence indicating a dominant role of any of these channel regions in neurotoxin binding. Moreover, relatively little of the overall energy of the toxin and sodium channel binding has been accounted for. Therefore, it is expected that peptides corresponding to each of these three sodium channel regions will exhibit only weak binding to scorpion toxins. In this study, we have shown that peptides corresponding to the sodium channel D4/S3−S4 loop exhibit an ∼1 mM affinity for LqhαIT. This corresponds to a $\Delta G°$ of ≈−4 kcal/mol, approximately one-third of the binding energy of toxin−insect Na$_v$ binding ($\Delta G° \approx -12$ kcal/mol for $K_d \approx 1$ nM). Despite this low binding affinity, the D4/S3−S4 segment, which has been implicated in scorpion toxin binding, resulted in specific and localized changes in LqhαIT chemical shifts upon binding. Moreover, it binds in a concentration-dependent manner that can be fit to a saturable curve compatible with a single binding event. These observations, together with the result of the control experiment with CTP3, led us to conclude that the binding is specific. Furthermore, our results are in good agreement with the results of site-directed mutagenesis discussed below, providing further evidence for specific binding.

*Domains of LqhαIT that Interact with the Na$_v$ D4/S3−S4 Loop.* Site-directed mutagenesis studies of both sodium channel and scorpion toxin provided information about which residues on each protein participate in binding. However, it is not known which domain in the scorpion toxin interacts with which region in the sodium channel. Here by using a set of D4/S3−S4 peptides, we clearly demonstrate that the D4/S3−S4 extracellular linker of the sodium channel interacts with the five-residue turn ($^{Lq}$K8−C12) and residues in its vicinity and with $^{Lq}$R58 at the C-terminal tail of LqhαIT.

The most noticeable changes in chemical shift upon titration of LqhαIT with the D4/S3−S4-derived peptides occurred for $^{Lq}$K8 and $^{Lq}$V13, detected via their backbone cross-peaks, and for $^{Lq}$R58, detected via its N$\epsilon$ side chain cross-peak. Addition of the longer peptide, SS($^{NaC}$S$_{1693}$−T$_{1711}$)GSS, resulted in the most pronounced changes in chemical shifts of LqhαIT despite the fact that this peptide was added at approximately half of the maximum concentration of the other D4/S3−S4 peptides. The $K_d$ for this peptide could not be determined due to its poor solubility in comparison with those of the shorter D4/S3−S4 peptides, for which $K_d$ could be determined. Chemical shift changes for residues $^{Lq}$K8, $^{Lq}$V13, and $^{Lq}$R58 were more pronounced upon addition of SS($^{NaC}$S$_{1693}$−T$_{1711}$)GSS peptide to LqhαIT, probably as a result of tighter interaction that could be due to stabilization of the peptide conformation or due to additional interactions of the added residues, $^{Lq-1693}$SILGLVL$^{1699}$, with the toxin. Small but significant changes in chemical shifts were also observed for $^{Lq}$N9 and $^{Lq}$C12 that are part of the five-residue loop and for $^{Lq}$R18, $^{Lq}$W38, and $^{Lq}$A39. The intensity of the cross-peaks of $^{Lq}$-Y14, $^{Lq}$F17, $^{Lq}$R18, and $^{Lq}$D19 decreased considerably upon SS($^{NaC}$S$_{1693}$−T$_{1711}$)GSS binding (Figures 4 and 5). Higher-than-threshold CSDs were observed for $^{Lq}$R18 and $^{Lq}$Q37 also after the addition of the shorter D4/S3−S4 peptides DDG($^{NaC}$S$_{1700}$−T$_{1711}$)GDD and SSG($^{NaC}$S$_{1700}$−T$_{1711}$)GSS. These changes reveal a second surface that could be involved in sodium channel binding (Figure 6). Interestingly, residues $^{Lq}$R18 and $^{Lq}$W38 were previously recognized as being important for LqhαIT binding by mutagenesis studies (*29*). The $^{Lq}$A39L mutation did not decrease toxin activity (*29*), but it is possible that the alanine role was retained by replacement with leucine.

*$^{Lq}$V13, a Newly Identified Bioactive Residue.* Together, the two surfaces implicated by the HSQC measurements (Figure

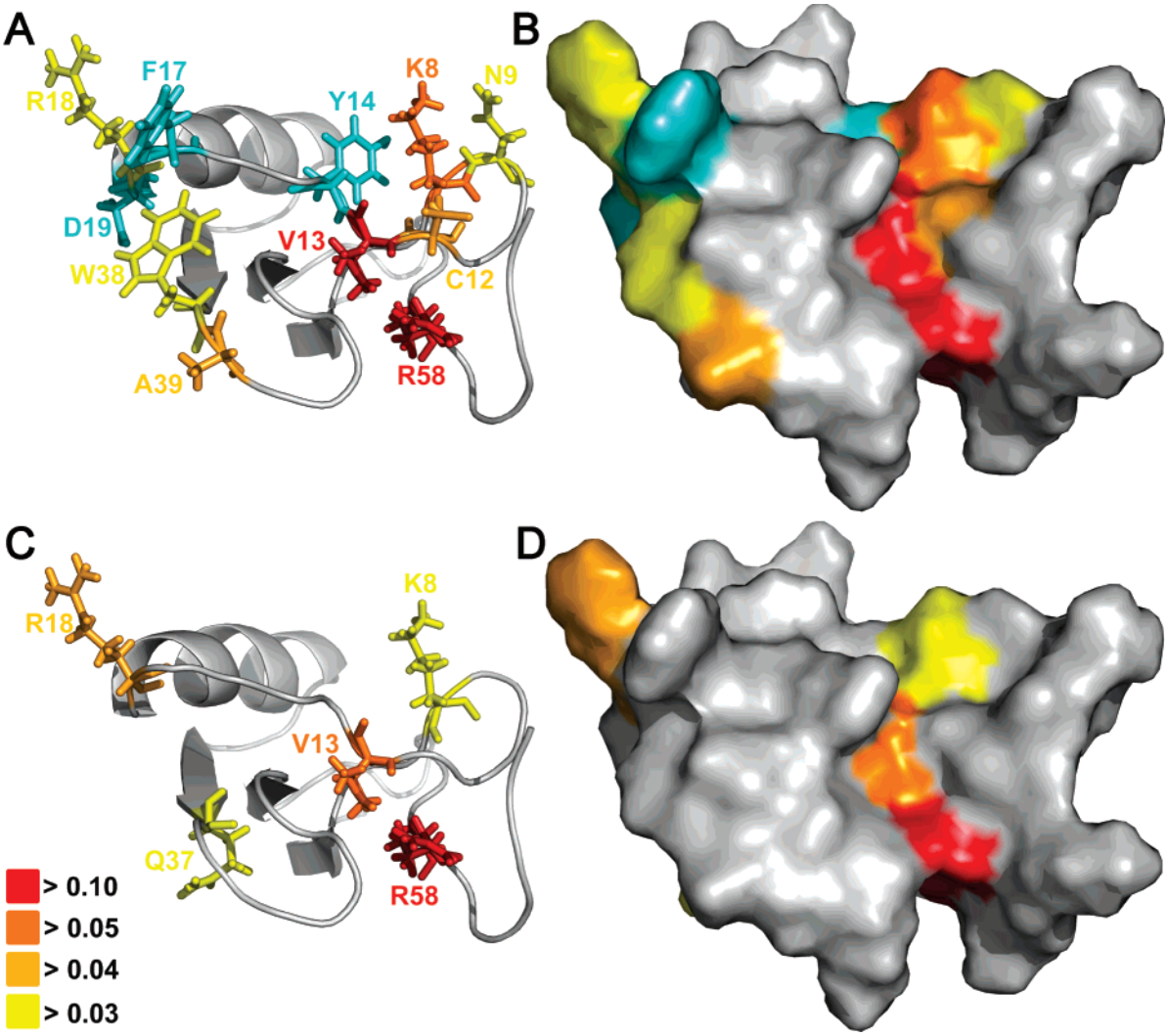


FIGURE 6: Mapping the LqhαIT binding site for the D4/S3−S4 peptides. Residues found to be involved in SS($^{NaC}S_{1693}$−$T_{1711}$)GSS binding are shown in stick (A) and surface (B) representations and are color-coded according to their CSD values. Residues found to be involved in SSG($^{NaC}S_{1700}$−$T_{1711}$)GSS binding are shown in stick (C) and surface (D) representations and are color-coded according to their CSD values. Residues that exhibited a considerable reduction in $^{1}H$−$^{15}N$ HSQC cross-peak intensity due to peptide binding are colored cyan. Two regions on the exterior of the molecule are formed.

6) in $Na_v$ binding partially overlap with two clusters on the LqhαIT exterior, which were previously identified by mutagenesis studies (*23*−*25*, *28*, *29*, *50*). However, the role of $^{Lq}$V13 in LqhαIT binding and activity has been revealed for the first time in this study, using NMR analysis, and was further corroborated by point mutagenesis. Conserved substitutions $^{Lq}$V13A and $^{Lq}$V13I or introduction of a polar group ($^{Lq}$V13T) markedly decreased the activity to insects, suggesting that $^{Lq}$V13 interacts with the channel receptor.

The role of $^{Lq}$N9 and $^{Lq}$C12 in toxin−receptor interaction has not been studied to date by site-directed mutagenesis due to their role in toxin structure (*27*). The involvement of these three residues in D4/S3−S4 binding, revealed by NMR, in addition to the previously recognized $^{Lq}$K8, suggests that the entire five-residue turn may undergo subtle changes upon interaction of the toxin with this channel region, which may also be influenced by residues on the structurally linked C-tail of the toxin which is also implicated in binding of $Na_v$s (*29*).

Despite the excellent agreement between NMR and mutagenesis studies, other residues which were formerly identified by mutagenesis to be important for binding, i.e., $^{Lq}$Y10, $^{Lq}$N44, and especially residues in the C-tail region ($^{Lq}$I57, $^{Lq}$V59, $^{Lq}$K62, and $^{Lq}$R64) (*28*, *29*), were not identified in our study as being involved in sodium channel binding. These discrepancies could mean that some of the binding residues in the toxin interact with a $Na_v$ binding determinant other than the D4/S3−S4 loop.

*The Regions Involved in D4/S3−S4 Binding Are Flexible in Free LqhαIT.* In a paper describing the determination of the structure of LqhαIT, we pointed out a few regions in which the atomic rmsd distribution with respect to the mean structure was higher, probably due to increased flexibility. The residues of LqhαIT found to be involved in binding of the D4/S3−S4 loop are localized to the more flexible domains of the toxin molecule. Among these regions are the five-residue turn comprised of residues $^{Lq}$K8−C12, residues $^{Lq}$Y16 and $^{Lq}$F17, the $^{Lq}$W38−G43 type I turn, and the C-terminus (*27*). This correlation suggests that flexibility could be important for binding and improve the fit between the toxin and the $Na_v$ target.

*Mode of Scorpion Toxin Binding with the Sodium Channel.* The bioactive surface of LqhαIT was suggested to be composed of two structurally distinct domains: the NC domain, consisting of the five-residue turn ($^{Lq-8}$KNYNC$^{12}$)

and the C-tail ($^{Lq-56}$PIRVPGKCR$^{64}$), and the Core domain (residues $^{Lq}$F17, $^{Lq}$R18, $^{Lq}$W38, and $^{Lq}$N44) (*29*). It was hypothesized that the Core domain participates in an anchoring interaction of the toxin with the receptor; that is, it enables the recognition of receptor site 3 by all toxins of the α-group. The NC domain, which varies in amino acid composition and spatial arrangement among α-toxin subgroups, was suggested to interact with another region of $Na_V$ and confers high binding affinity (*29*).

Our study suggests that the two domains previously shown to compose the bioactive surface of LqhαIT (the NC and Core domains) may be functionally divided in a different manner according to their contribution to the $Na_v$ binding. Of the five-residue turn residues, which are part of the previously suggested NC domain (*29*), $^{Lq}$K8, $^{Lq}$N9, and the newly identified adjacent residues, $^{Lq}$C12 and $^{Lq}$V13, are thought to make up part of an interacting surface, together with $^{Lq}$R18 and $^{Lq}$W38 of the Core domain. This surface interacts with the D4/S3−S4 loop. The other bioactive residues in the C-tail region ($^{Lq}$I57, $^{Lq}$V59, $^{Lq}$K62, and $^{Lq}$R64) may interact with other parts of the channel receptor, outside of the D4/S3−S4 region.

In this study, the conformation of the bound sodium channel peptide has not been determined due to the weak binding affinity which, at the moment, does not enable structure determination by isotope-filtered or transferred NOE experiments. It should be noted that in similar studies of interactions of chemokine with N-terminal peptides of CXCR4 and CCR5, the conformation of the bound peptide has not been determined and NOE interactions were not detected between the protein and the peptide (*51*, *52*).

This study provides a unique perspective on the toxin−sodium channel binding interface and demonstrates the complementarity between structural studies by NMR and biochemical research. Ongoing attempts to set up an expression system for the D4/S3−S4 peptides will permit identification of the peptide's residues participating in the interaction with $Na_v$s and, more interestingly, investigation of the different peptides' conformations. Additional studies exploring other extracellular regions of the sodium channel are required to further characterize the binding site of LqhαIT on $Na_v$s. Such studies of the LqhαIT−channel binding site at the molecular level could shed light on the toxin−receptor interaction and reveal molecular details that underlie the ability of the toxin to distinguish among $Na_v$ subtypes. Furthering our understanding of the molecular mechanisms underlying the sodium channel−toxin binding interactions will also offer new insight into the channel gating mechanism.

## ACKNOWLEDGMENT

We thank Mr. M. Ben-David and Mr. E. Noah for their help in peptide expression and Mr. Y. Hayek for help in purification of peptides. Useful comments and suggestions of Dr. T. Scherf and Dr. N. Kessler are gratefully acknowledged.

## SUPPORTING INFORMATION AVAILABLE

Effect of $^{Lq}$V13 substitution on LqhαIT activity at the insect sodium channel $DmNa_v1$. This material is available free of charge via the Internet at http://pubs.acs.org.

## REFERENCES

1. Catterall, W. A. (2000) From ionic currents to molecular mechanisms: The structure and function of voltage-gated sodium channels, *Neuron 26*, 13−25.
2. Cestele, S., and Catterall, W. A. (2000) Molecular mechanisms of neurotoxin action on voltage-gated sodium channels, *Biochimie 82*, 883−892.
3. Domene, C., Haider, S., and Sansom, M. S. (2003) Ion channel structures: A review of recent progress, *Curr. Opin. Drug Discovery Dev. 6*, 611−619.
4. Catterall, W. A. (2001) A 3D view of sodium channels, *Nature 409*, 988−991.
5. Hubner, C. A., and Jentsch, T. J. (2002) Ion channel diseases, *Hum. Mol. Genet. 11*, 2435−2445.
6. Wada, A. (2006) Roles of voltage-dependent sodium channels in neuronal development, pain, and neurodegeneration, *J. Pharmacol. Sci. 102*, 253−268.
7. Qu, Y., Curtis, R., Lawson, D., Gilbride, K., Ge, P., DiStefano, P. S., Silos-Santiago, I., Catterall, W. A., and Scheuer, T. (2001) Differential modulation of sodium channel gating and persistent sodium currents by the β1, β2, and β3 subunits, *Mol. Cell. Neurosci. 18*, 570−580.
8. Yu, F. H., Westenbroek, R. E., Silos-Santiago, I., McCormick, K. A., Lawson, D., Ge, P., Ferriera, H., Lilly, J., DiStefano, P. S., Catterall, W. A., Scheuer, T., and Curtis, R. (2003) Sodium channel β4, a new disulfide-linked auxiliary subunit with similarity to β2, *J. Neurosci. 23*, 7577−7585.
9. Rogers, J. C., Qu, Y., Tanada, T. N., Scheuer, T., and Catterall, W. A. (1996) Molecular determinants of high affinity binding of α-scorpion toxin and sea anemone toxin in the S3−S4 extracellular loop in domain IV of the $Na^+$ channel α subunit, *J. Biol. Chem. 271*, 15950−15962.
10. Yang, N., George, A. L., Jr., and Horn, R. (1996) Molecular basis of charge movement in voltage-gated sodium channels, *Neuron 16*, 113−122.
11. Sheets, M. F., Kyle, J. W., Kallen, R. G., and Hanck, D. A. (1999) The Na channel voltage sensor associated with inactivation is localized to the external charged residues of domain IV, S4, *Biophys. J. 77*, 747−757.
12. West, J. W., Patton, D. E., Scheuer, T., Wang, Y., Goldin, A. L., and Catterall, W. A. (1992) A cluster of hydrophobic amino acid residues required for fast $Na^+$-channel inactivation, *Proc. Natl. Acad. Sci. U.S.A. 89*, 10910−10914.
13. Wang, S. Y., and Wang, G. K. (2003) Voltage-gated sodium channels as primary targets of diverse lipid-soluble neurotoxins, *Cell. Signalling 15*, 151−159.
14. Salceda, E., Garateix, A., and Soto, E. (2002) The sea anemone toxins BgII and BgIII prolong the inactivation time course of the tetrodotoxin-sensitive sodium current in rat dorsal root ganglion neurons, *J. Pharmacol. Exp. Ther. 303*, 1067−1074.
15. Gordon, D., Martin-Eauclaire, M. F., Cestele, S., Kopeyan, C., Carlier, E., Khalifa, R. B., Pelhate, M., and Rochat, H. (1996) Scorpion toxins affecting sodium current inactivation bind to distinct homologous receptor sites on rat brain and insect sodium channels, *J. Biol. Chem. 271*, 8034−8045.
16. Tejedor, F. J., and Catterall, W. A. (1988) Site of covalent attachment of α-scorpion toxin derivatives in domain I of the sodium channel α subunit, *Proc. Natl. Acad. Sci. U.S.A. 85*, 8742−8746.
17. Thomsen, W. J., and Catterall, W. A. (1989) Localization of the receptor site for α-scorpion toxins by antibody mapping: Implications for sodium channel topology, *Proc. Natl. Acad. Sci. U.S.A. 86*, 10161−10165.
18. Cestele, S., Yarov-Yarovoy, V., Qu, Y., Sampieri, F., Scheuer, T., and Catterall, W. A. (2006) Structure and function of the voltage sensor of sodium channels probed by a β-scorpion toxin, *J. Biol. Chem. 281*, 21332−21344.
19. Strugatsky, D., Zilberberg, N., Stankiewicz, M., Ilan, N., Turkov, M., Cohen, L., Pelhate, M., Gilles, N., Gordon, D., and Gurevitz, M. (2005) Genetic polymorphism and expression of a highly potent scorpion depressant toxin enable refinement of the effects on insect Na channels and illuminate the key role of Asn-58, *Biochemistry 44*, 9179−9187.
20. Possani, L. D., Becerril, B., Delepierre, M., and Tytgat, J. (1999) Scorpion toxins specific for $Na^+$-channels, *Eur. J. Biochem. 264*, 287−300.
21. Gurevitz, M., Karbat, I., Cohen, L., Ilan, N., Kahn, R., Turkov, M., Stankiewicz, M., Stuhmer, W., Dong, K., and Gordon, D.

(2007) The insecticidal potential of scorpion *β*-toxins, *Toxicon 49*, 473−489.
22. Leipold, E., Lu, S., Gordon, D., Hansel, A., and Heinemann, S. H. (2004) Combinatorial interaction of scorpion toxins Lqh-2, Lqh-3, and LqhαIT with sodium channel receptor sites-3, *Mol. Pharmacol. 65*, 685−691.
23. Gordon, D., and Gurevitz, M. (2003) The selectivity of scorpion α-toxins for sodium channel subtypes is determined by subtle variations at the interacting surface, *Toxicon 41*, 125−128.
24. Gordon, D., Kallen, R. G., and Heinemann, S. H. (2004) Sodium channel features that confer differential sensitivity to various scorpion α-toxins, in *Neurotox '03: Neurotoxicological Targets from Functional Genomics and Proteomics* (Beadle, D. J., Mellor, I. R., and Usherwood, P. N. R., Eds.) Society of Chemical Industry, London.
25. Gordon, D., Karbat, I., Ilan, N., Cohen, L., Kahn, R., Gilles, N., Dong, K., Stuhmer, W., Tytgat, J., and Gurevitz, M. (2007) The differential preference of scorpion α-toxins for insect or mammalian sodium channels: Implications for improved insect control, *Toxicon 49*, 452−472.
26. Eitan, M., Fowler, E., Herrmann, R., Duval, A., Pelhate, M., and Zlotkin, E. (1990) A scorpion venom neurotoxin paralytic to insects that affects sodium current inactivation: Purification, primary structure, and mode of action, *Biochemistry 29*, 5941−5947.
27. Tugarinov, V., Kustanovich, I., Zilberberg, N., Gurevitz, M., and Anglister, J. (1997) Solution structures of a highly insecticidal recombinant scorpion α-toxin and a mutant with increased activity, *Biochemistry 36*, 2414−2424.
28. Zilberberg, N., Froy, O., Loret, E., Cestele, S., Arad, D., Gordon, D., and Gurevitz, M. (1997) Identification of structural elements of a scorpion α-neurotoxin important for receptor site recognition, *J. Biol. Chem. 272*, 14810−14816.
29. Karbat, I., Frolow, F., Froy, O., Gilles, N., Cohen, L., Turkov, M., Gordon, D., and Gurevitz, M. (2004) Molecular basis of the high insecticidal potency of scorpion α-toxins, *J. Biol. Chem. 279*, 31679−31686.
30. Leipold, E., Hansel, A., Olivera, B. M., Terlau, H., and Heinemann, S. H. (2005) Molecular interaction of *δ*-conotoxins with voltage-gated sodium channels, *FEBS Lett. 579*, 3881−3884.
31. Karbat, I., Kahn, R., Cohen, L., Ilan, N., Gilles, N., Corzo, G., Froy, O., Gur, M., Albrecht, G., Heinemann, S. H., Gordon, D., and Gurevitz, M. (2007) The unique pharmacology of the scorpion α-like toxin Lqh3 is associated with its flexible C-tail, *FEBS J. 274*, 1918−1931.
32. Sato, C., Ueno, Y., Asai, K., Takahashi, K., Sato, M., Engel, A., and Fujiyoshi, Y. (2001) The voltage-sensitive sodium channel is a bell-shaped molecule with several cavities, *Nature 409*, 1047−1051.
33. Basus, V. J., Song, G., and Hawrot, E. (1993) NMR solution structure of an α-bungarotoxin/nicotinic receptor peptide complex, *Biochemistry 32*, 12290−12298.
34. Samson, A., Scherf, T., Eisenstein, M., Chill, J., and Anglister, J. (2002) The mechanism for acetylcholine receptor inhibition by α-neurotoxins and species-specific resistance to α-bungarotoxin revealed by NMR, *Neuron 35*, 319−332.
35. Scherf, T., Hiller, R., Naider, F., Levitt, M., and Anglister, J. (1992) Induced peptide conformations in different antibody complexes: Molecular modeling of the three-dimensional structure of peptide-antibody complexes using NMR-derived distance restraints, *Biochemistry 31*, 6884−6897.
36. Biron, Z., Khare, S., Quadt, S. R., Hayek, Y., Naider, F., and Anglister, J. (2005) The 2F5 Epitope Is Helical in the HIV-1 Entry Inhibitor T-20, *Biochemistry 44*, 13602−13611.
37. Bornstein, P., and Balian, G. (1977) Cleavage at Asn-Gly bonds with hydroxylamine, *Methods Enzymol. 47*, 132−145.
38. Li-Smerin, Y., and Swartz, K. J. (2001) Helical structure of the COOH terminus of S3 and its contribution to the gating modifier toxin receptor in voltage-gated ion channels, *J. Gen. Physiol. 117*, 205−218.
39. Nguyen, T. P., and Horn, R. (2002) Movement and crevices around a sodium channel S3 segment, *J. Gen. Physiol. 120*, 419−436.
40. Zilberberg, N., Gordon, D., Pelhate, M., Adams, M. E., Norris, T. M., Zlotkin, E., and Gurevitz, M. (1996) Functional expression and genetic alteration of an α scorpion neurotoxin, *Biochemistry 35*, 10215−10222.
41. Shichor, I., Zlotkin, E., Ilan, N., Chikashvili, D., Stuhmer, W., Gordon, D., and Lotan, I. (2002) Domain 2 of *Drosophila* para voltage-gated sodium channel confers insect properties to a rat brain channel, *J. Neurosci. 22*, 4364−4371.
42. Moran, Y., Cohen, L., Kahn, R., Karbat, I., Gordon, D., and Gurevitz, M. (2006) Expression and mutagenesis of the sea anemone toxin Av2 reveals key amino acid residues important for activity on voltage-gated sodium channels, *Biochemistry 45*, 8864−8873.
43. Delaglio, F., Grzesiek, S., Vuister, G. W., Zhu, G., Pfeifer, J., and Bax, A. (1995) NMRPipe: A multidimensional spectral processing system based on UNIX pipes, *J. Biomol. NMR 6*, 277−293.
44. Johnson, B. A., and Blevins, R. A. (1994) NMR View: A Computer-Program for the Visualization and Analysis of NMR Data, *J. Biomol. NMR 4*, 603−614.
45. Johnson, B. A. (2004) Using NMRView to visualize and analyze the NMR spectra of macromolecules, *Methods Mol. Biol. 278*, 313−352.
46. Shuker, S. B., Hajduk, P. J., Meadows, R. P., and Fesik, S. W. (1996) Discovering high-affinity ligands for proteins: SAR by NMR, *Science 274*, 1531−1534.
47. Zuiderweg, E. R. (2002) Mapping protein-protein interactions in solution by NMR spectroscopy, *Biochemistry 41*, 1−7.
48. Nietlispach, D., Mott, H. R., Stott, K. M., Nielsen, P. R., Thiru, A., and Laue, E. D. (2004) Structure determination of protein complexes by NMR, *Methods Mol. Biol. 278*, 255−288.
49. Gilles, N., Krimm, I., Bouet, F., Froy, O., Gurevitz, M., Lancelin, J. M., and Gordon, D. (2000) Structural implications on the interaction of scorpion α-like toxins with the sodium channel receptor site inferred from toxin iodination and pH-dependent binding, *J. Neurochem. 75*, 1735−1745.
50. Gurevitz, M., Gordon, D., Ben-Natan, S., Turkov, M., and Froy, O. (2001) Diversification of neurotoxins by C-tail 'wiggling': A scorpion recipe for survival, *FASEB J. 15*, 1201−1205.
51. Gozansky, E. K., Louis, J. M., Caffrey, M., and Clore, G. M. (2005) Mapping the binding of the N-terminal extracellular tail of the CXCR4 receptor to stromal cell-derived factor-1α, *J. Mol. Biol. 345*, 651−658.
52. Duma, L., Haussinger, D., Rogowski, M., Lusso, P., and Grzesiek, S. (2007) Recognition of RANTES by extracellular parts of the CCR5 receptor, *J. Mol. Biol. 365*, 1063−1075.

BI701323K